MEASUREMENT OF WALL TEMPERATURE FLUCTUATIONS DURING THERMAL MIXING OF NON-ISOTHERMAL WATER STREAMS

H. Anglart, M. Bergagio, S. Hedberg and S. Rydström
KTH Royal Institute of Technology
Roslagstullsbacken 21, 10691 Stockholm, Sweden
henryk@kth.se; bergagio@kth.se; stellan.hedberg@energy.kth.se; stefan@particle.kth.se

W. Frid
Swedish Radiation Safety Authority
Solna Strandväg 96
171 16 Stockholm, Sweden
wiktor.frid@ssm.se

ABSTRACT

This paper is dealing with measurement of temperature fluctuations during mixing of two water streams in an annular test section at BWR operational conditions. The experiments are simulating conditions existing in a guide tube of BWR control rods, where relatively cold water at about 333 K is mixing with hot water at ~550 K. It is shown that the mixing is causing high amplitude temperature fluctuations in the solid walls of the control rod extender. Using new movable multi-sensors it became possible to obtain a large experimental database, containing wall temperature measurements at 8 azimuthal and 5 axial positions, with 13 thermocouples at each position. In total 520 temperature readings were performed, each lasting about 2 minutes and recording transient temperature with frequency of at least 100 samples per second and with estimated non-calibrated uncertainty less than 3.9 K. The present experimental results can be used to analyze the governing phenomena during thermal mixing and also to validate CFD conjugate heat transfer models of thermal mixing applied to actual reactor geometries.

1. INTRODUCTION

Thermal fatigue is one of the six main ageing mechanisms that are commonly considered in evaluation of the reduction of the lifetime of the piping components in the reactor coolant system. This phenomenon is highly relevant to all components in nuclear power plants where mixing of two non-isothermal streams may occur such as in surge, spray and branch lines. Three governing phenomena which are causing thermal fatigue in surge lines and nozzles are the thermal stratification, the thermal stripping and the thermal shocks.

Global thermal stratification is a term used to describe a low-cycle process of changing conditions from stratification to no-stratification and back to stratification again. Usually this type of thermal stratification is resulting with macroscopic displacements of the pipe. Cyclic thermal stratification is a term used to describe changes in the elevation of the interface between the hot and the cold fluid. This type of thermal

stratification is associated with cyclic through-wall bending stresses that cause fatigue damages without any macroscopic displacement of the pipe.

Thermal striping is a process in which stresses in a wall are created by oscillations of the fluid temperature at the interface between hot and cold fluids. The process can be related to presence of Kelvin-Helmholtz instability, when inertial forces overcome stratifying density differences between the fluid layers.

Thermal fatigue in nuclear power plants was initially investigated in connection to Liquid-Metal Fast Breeder Reactors (LMFBRs), where significant damage risks due to it could be expected. Soon the attention was shifted to Light Water Reactors (LWRs) due to several failure events in various countries such as France (mixing tees of residual heat removal system at Civaux 1), Japan (regenerative heat exchangers at Tsuruga and Tomari) and USA (safety injection dead leg at Farley) [1].

A related event took place recently in BWRs in Sweden. During the 2008 refueling outage at Oskarshamn 3 reactor it was found that one control rod extender was completely broken and several had incipient cracks. Shortly after a similar problem was identified at Forsmark 3 reactor, which is of similar design as Oskarshamn 3 reactor. Inspections and tests at both reactors revealed that about 37% of all control rod extenders suffered from cracks.

A common feature of both plants is that the temperature of the purge flow through the control rod actuators is about 333.15 K (60 °C), whereas the temperature of the surrounding reactor water is about 549.15 K (276 °C).

Analyses indicate that in guide tubes of control rods the streams have the following mass flow rates: 0.07 kg/s for the cold purge flow and 11.77 kg/s for the hot reactor flow [2]. The purge flow through the actuators cools them and prevents the build-up of crud. Because of the substantial temperature difference between the purge flow and the reactor water, the purge flow can cause thermal fatigue resulting from thermal stresses due to high temperature differences.

In a wake of control rod problems at Oskarshamn 3 and Forsmark 3 reactors, investigations of the possible causes were undertaken [2, 3]. Experimental investigations of flow mixing inside a control-rod guide tube was performed [3]. Two full-scale mockups were developed, one operating at atmospheric pressure and with ΔT approximately equal to 30 K for visualization of the mixing process and one operating at elevated pressure and providing ΔT equal to 80 K. The measurements showed that the mixing zone between the hot and cold streams is characterized by low frequency and high amplitude temperature fluctuations. The velocity fluctuations were also very large as compared to the mean bulk velocity [3].

An attempt was made to extrapolate the measured results from experimental conditions to reactor conditions using the dimensional analysis [3]. It was concluded that the temperature oscillations should have amplitudes up to the whole temperature difference between the hot and cold streams, and should be dominated by low frequencies, of the order of 0.1 Hz [3]. The present experiments were designed to confirm the previously obtained results at operational conditions similar to those encountered in BWRs.
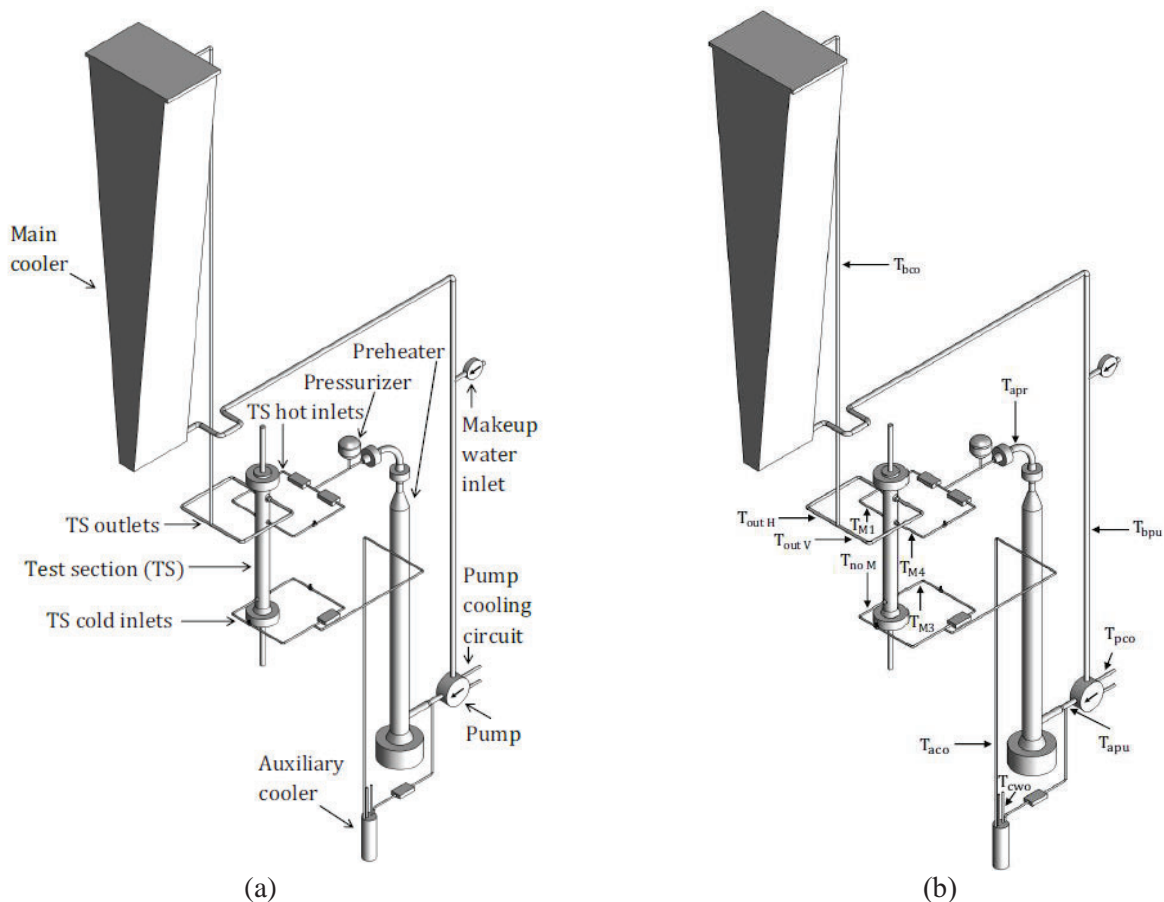

2. EXPERIMENT

One of the main objectives of the current project is to perform thermal-mixing experiments at the same pressure and temperature levels as encountered in the guide tubes of BWR control rods. To achieve this, the HWAT (High-pressure Water Test) loop at the Royal Institute of Technology has been adopted and a dedicated test section was constructed. Both the loop and the test-section have been well instrumented to

provide detailed information about the boundary conditions and mixing characteristics in the test section. These following sections contain a detailed description of the performed experiments.

2.1. Experimental facility

Figures 1 (a) and (b) show a schematic of the experimental loop and its major components, together with locations of loop thermocouples. The working fluid (water at 7.2 MPa) is flowing through the preheater, the test section and the main cooler using the main circulation loop. A fraction of the working fluid is bypassing the preheater and is flowing through an auxiliary cooler to provide the cold stream at the required exit temperature, which is next entering the test section at the bottom. To damp possible pressure fluctuations, a pressurizer has been installed at the hot leg, between the preheater and the hot inlets to the test section (Fig. 1a).

(a)   (b)

Figure 1. A schematic of the experimental loop: (a) main loop components; (b) locations of loop thermocouples; T_{apu} – temperature at the outlet from the pump, T_{aco} – temperature of the cold stream, T_{cwo} – outlet temperature of water on the secondary side of the cooler, T_{M3} – temperature of the cold inlet stream in leg 2, T_{noM} - temperature of the cold inlet stream in leg 1, T_{apr} – temperature of the hot stream, T_{M1} – temperature of the hot inlet stream in leg 1, T_{M4} – temperature of the hot inlet stream in leg 2, T_{outH} – temperature of the outlet stream in leg 1, T_{outV} – temperature of the outlet stream in leg 2, T_{bco} – temperature of the outlet stream.

The test section consists of two stainless steel concentric tubes with annular volume in between with dimensions 35x80x1150 mm, closed with two sealed flanges at the bottom and the top of the test section.

The outer tube (Fig. 2), made of austenitic stainless steel and with dimensions 80x100x1150 mm, constitutes a pressure vessel in which the mixing takes place and which is designed to withstand 7.2 MPa pressure. The tube has 6 orifices: two cold inlet orifices with inner diameter 7.5 mm each, two hot inlet orifices with inner diameter 7.5 mm each and two outlet orifices with inner diameter 14 mm each. Whereas the outer tube is fixed, the inner tube can rotate and move up and down to increase the measurement range (Fig. 3).
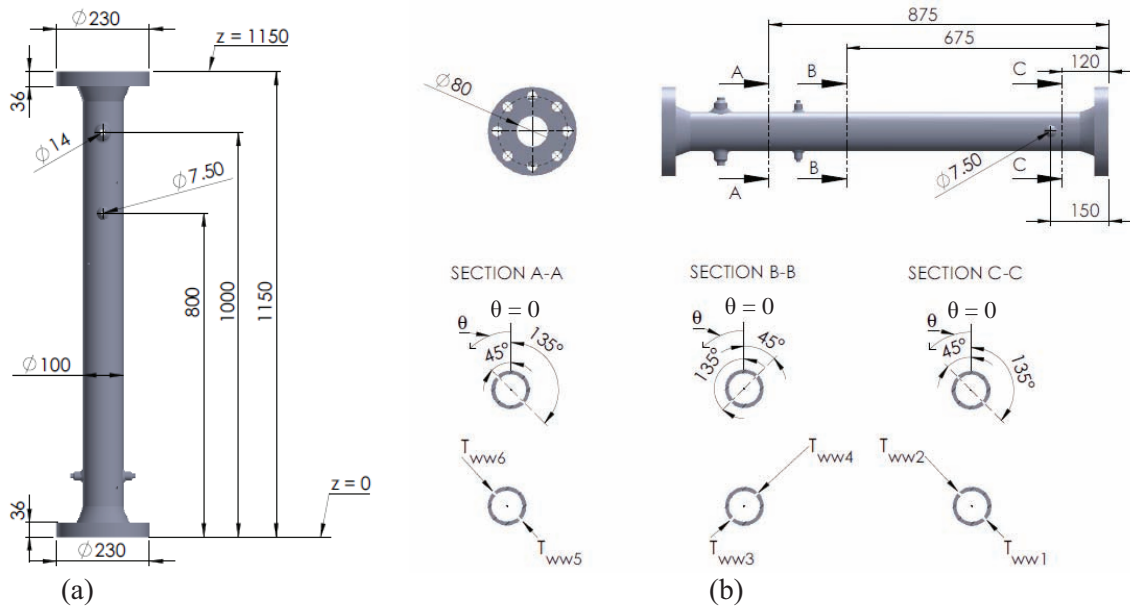
Figure 2. Outer tube of the test section: (a) main dimensions and location of hot inlet and exit orifices; (b) location cold inlet orifices and thermocouples.
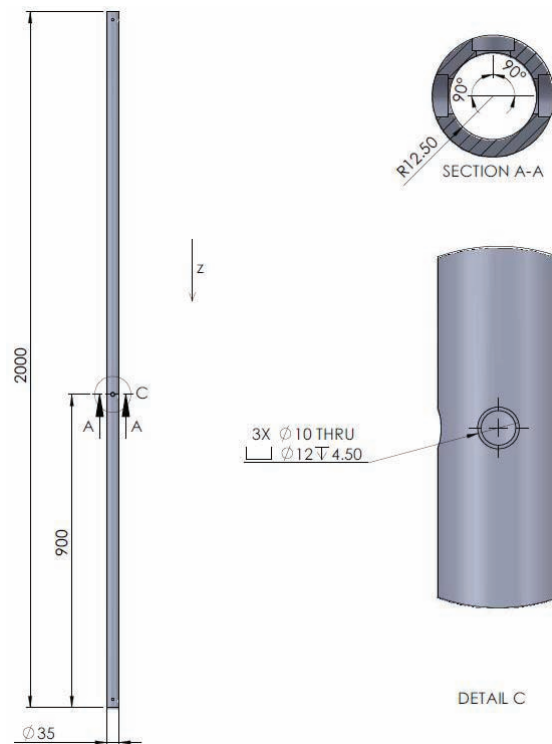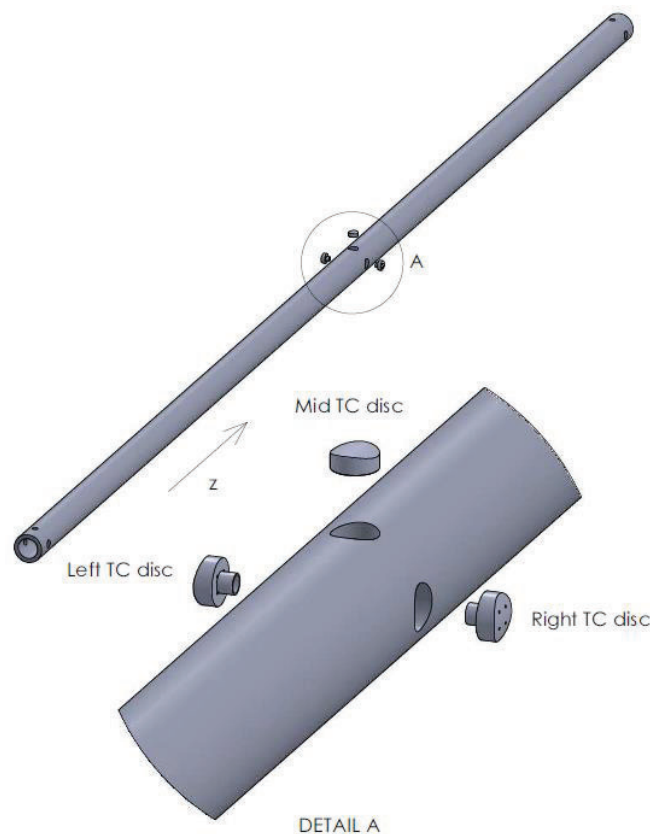

Figure 3. Inner tube of the test section with three thermocouple discs shown in cross-section A-A.

The inner tube (called also a stem in this paper) is made of austenitic stainless steel and has dimensions 25 x 35 x 2000 mm. It can be freely moved in the z-direction and rotated in the θ-direction using a step motor and a hydraulic actuator. In the upper and lower parts of the test section, the inner tube is penetrating through flanges closing the test section mixing volume from the top and the bottom. The penetrations are sealed to prevent water leakages from the test section during the loop operation at high pressure. The inner tube contains three discs, which are housing thermocouples (further referred to as "thermocouple discs" or TC discs), as shown in Figs. 3 and 4.

The convention used in the naming of the thermocouple discs is shown in Fig. 4. The geometry of the left and right TC discs is shown in Fig. 5a. Both these TC discs were designed identical, however, due to assembling issues, they contain different numbers of active thermocouples. The discs contain thermocouples that completely penetrate the wall and are designed to measure the wet surface temperature. In addition, one thermocouple in each disc is attached to the inner surface to provide a reference dry surface temperature. Similarly, Fig. 5b shows the geometry details of the mid TC disc, which is housing thermocouples submerged at different depths in the wall material.

Figure 4. Inner tube of the test section with three thermocouple (TC) discs shown in cross-section A-A.

As shown in Fig. 5, the left and right thermocouple discs (further referenced as T_Vn and T_Hn, respectively, where n is the thermocouple identification number) are designed to measure the wall surface temperature. Wall surface thermocouples similar to the one used for measurement of a transient wall heat flux under diesel engine conditions is employed [4]. This type of arrangement allows for an analytical evaluation of the heat flux [5]. In addition, the thermocouple is not perturbing the flow around it and thus

provides the true wall surface temperature. The central thermocouple disc (further referenced T_C*n*) is designed to measure the temperature distribution inside wall at five different depths of the wall material.
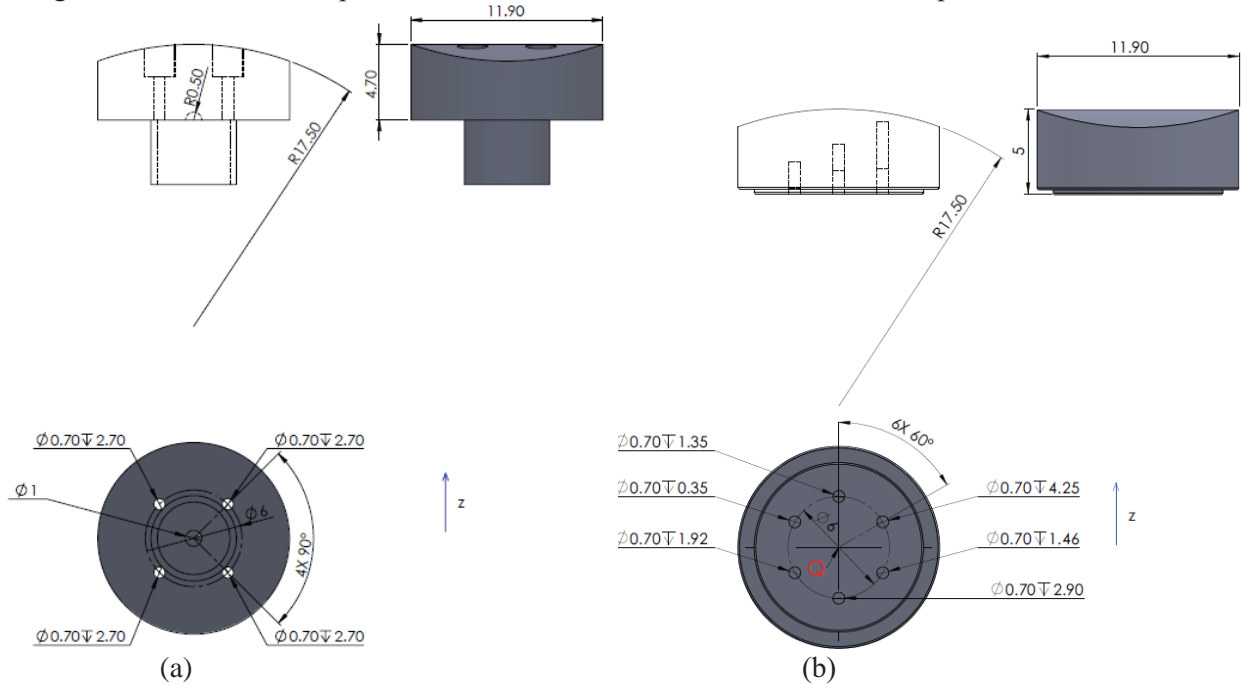

(a)   (b)

Figure 5. Geometry details of TC discs: (a) left and right TC disc; (b) mid TC disc.

Figure 6 shows labels of the thermocouples that were active during experiments, whereas Table I contains their precise positions. As a reference, the azimuthal and the axial positions of the center of the mid TC disc are designed as θ_Q, and z_Q, respectively.
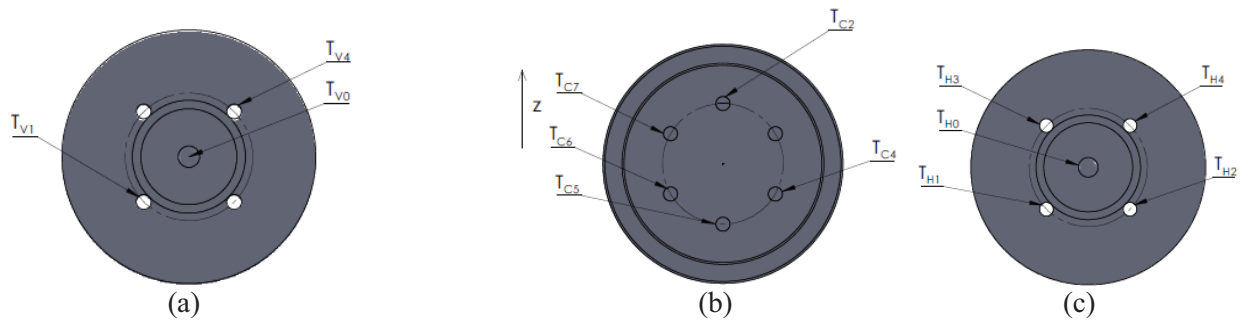

(a)   (b)   (c)

Figure 6. Thermocouple labels in the movable stem: (a) left TC disc; (b) mid TC disc; (c) right TC disc.

Table I. Location of thermocouples in the test section (θ_Q, z_Q – coordinates of the center of mid TC disc; see Fig. 2 for definition of z = 0 and θ = 0).

TC	r[mm]	θ [°]	z [mm]
T_C2	13.85	θ_Q	z_Q +3
T_C4	14.20	$\theta_Q - 10.54°$	$z_Q - \delta^{2)}$
T_C5	15.40	θ_Q	z_Q -3
T_C6	14.65	$\theta_Q + 10.21°$	$z_Q - \delta^{2)}$

T_C7	13.11	$\theta_Q + 11.43°$	$z_Q + \delta$ [2]
T_V0	13.30	$\theta_Q - 90°$	z_Q
T_V1	17.50	$\theta_Q - 90°+\alpha$ [1]	$z_Q -\lambda$ [3]
T_V4	17.50	$\theta_Q - 90°-\alpha$ [1]	$z_Q +\lambda$ [3]
T_H0	13.30	$\theta_Q + 90°$	z_Q
T_H1	17.50	$\theta_Q + 90°+\alpha$ [1]	$z_Q -\lambda$ [3]
T_H2	17.50	$\theta_Q + 90°-\alpha$ [1]	$z_Q -\lambda$ [3]
T_H3	17.50	$\theta_Q + 90°+\alpha$ [1]	$z_Q +\lambda$ [3]
T_H4	17.50	$\theta_Q + 90°-\alpha$ [1]	$z_Q +\lambda$ [3]
T_{ww1}	40.00	225°	120
T_{ww2}	40.00	45°	120
T_{ww3}	40.00	135°	675
T_{ww4}	40.00	315°	675
T_{ww5}	40.00	225°	875
T_{ww6}	40.00	45°	875

[1] $\alpha \approx 6.95°$; [2] $\delta=3\cdot\sin(30°)=1.5$ mm; [3] $\lambda=3*\sin(45°) \approx 2.12$ mm.

2.2. Experimental conditions

All experiments have been performed at 7.2 MPa reference pressure, with variable flow rates and temperatures at hot and cold inlets, as indicated in Table II.

Table II. Experimental matrix.

| Case	Cold inlet flow, kg/s	Cold inlet temperature, K	Hot inlet flow, kg/s	Hot inlet temperature, K
1	0.07	333.15	0.8	549.15
6	0.07	423.15	0.6	549.15
9	0.07	333.15	0.4	549.15

2.3. Experimental procedures

At given experimental set point indicated in Table II, the inner stem was rotated between angles $\theta = 0°$ and $\theta = 360°$ with a step equal to about 45° and moved between axial locations $z_Q = 0.6$ m and $z_Q = 0.8$ m with a step equal to 0.05 m. This resulted in wall temperature measurements at 8 azimuthal and 5 axial positions, with 13 thermocouples at each position. In total 520 temperature readings have been performed, each lasting about 2 minutes and recording transient temperature with frequency of 100 samples per second. A thorough uncertainty analysis described in the companion paper [6] indicates that the instantaneous temperature was measured on average with non-calibrated uncertainty less than 3.9 K.
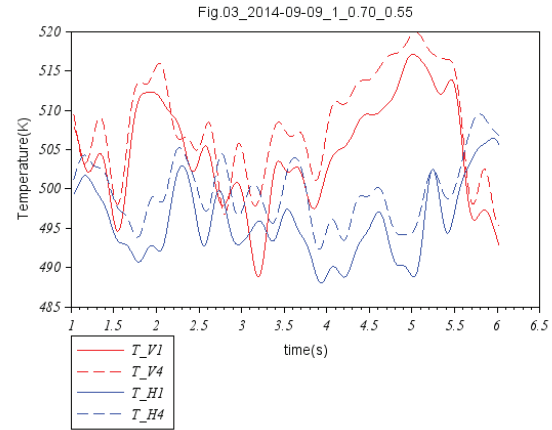
3. EXPERIMENTAL RESULTS

Sample measured temperature fluctuations at the left and right TC discs for the three cases included in Table II are shown in Fig. 7. The figures in the left column show the measured signal during
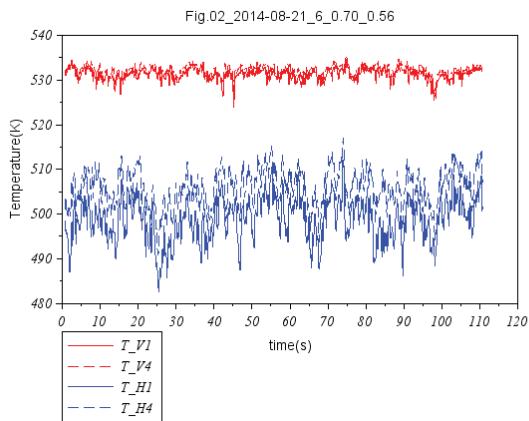
approximately 110 sec., whereas the figures in the right column show only the first 5 sec. of the measured signal.
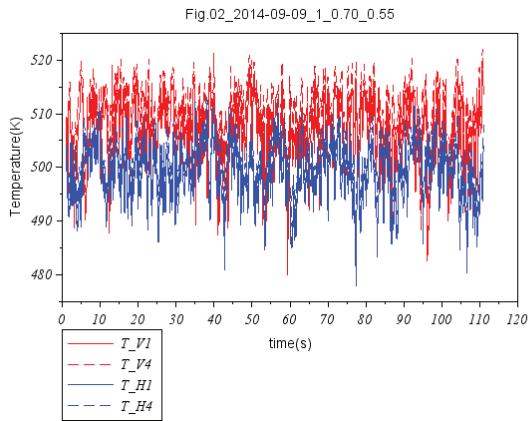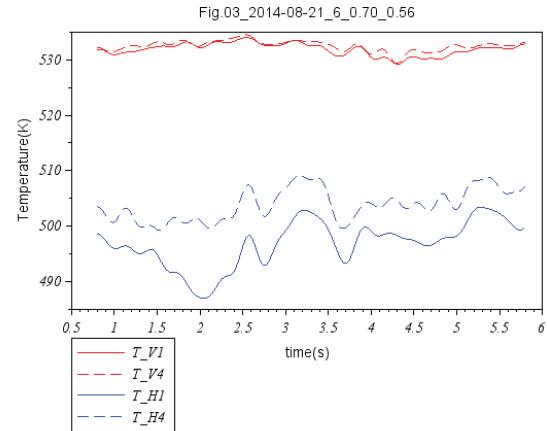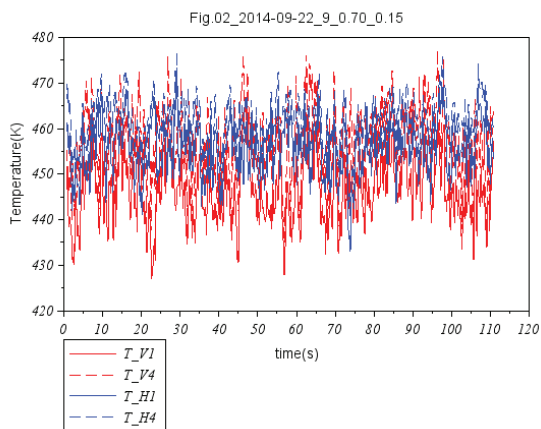

(a)

(b)
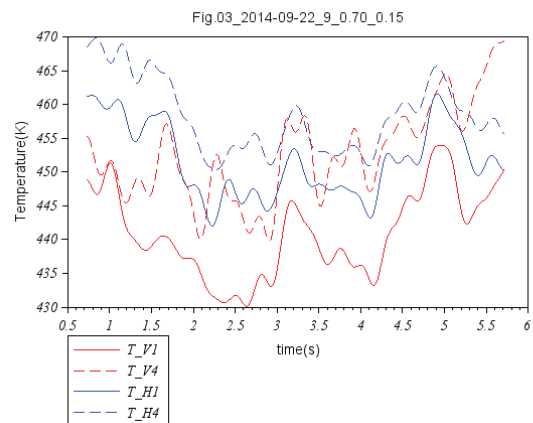

(c)

(d)

(e)

(f)

Figure 7. Measured temperature fluctuations at left TC disc (T_V1 and T_V4) and right TC disc (T_H1 and T_H4): (a) and (b) – case 1, axial location z_Q = 0.7 m, θ_Q = 0.55°; (c) and (d) – case 6, axial location z_Q = 0.7 m, θ_Q = 0.56°; (e) and (f) – case 9, axial location z_Q = 0.7 m, θ_Q = 0.15°;

Figures 7(a,b) show the wall surface temperature as a function of time for case 1 and at the axial location z = 700 mm (100 mm below the hot inlets), when the total cold flow rate is 0.07 kg/s and the total hot flow rate is 0.8 kg/s. Thermocouples T_V1 and T_V4, located approximately at – 90° angle from the hot inlet (that is in a plane perpendicular to the hot inlets) indicate temperature fluctuations at a level slightly higher than the temperatures at thermocouples T_H1 and T_H4, which are located approximately at +90° angle from the hot inlet. If the flow was perfectly symmetrical, the temperatures should oscillate around the same mean value.

A large temperature asymmetry manifest itself in Figs. 7(c,d) for case 6 with the total hot mass flow rate 0.6 kg/s, where the difference between the temperatures measured by V-thermocouples and H-thermocouples is as high as ~30 K. This asymmetry indicates that the hot stream penetrates one side of the stem on which V-thermocouples are installed, whereas the cold stream prevails on the other side of the stem. For case 9, when the total hot inlet flow rate is reduced to 0.4 kg/s, the distribution of temperatures at both sides of the stem (that is at V- and H-thermocouples) is again quite similar, with slightly higher mean temperature recorded by H-thermocouples.

The observed asymmetry of temperature distributions could be expected due to the location of two hot inlets exactly aligned and opposite to each other. This configuration is prone to large instabilities, since two water streams of equal momentum are competing with each other. However, explanations why this leads to asymmetry in temperature distribution only for selected flow rates will require further investigation.

Figures 8(a,b) show a distribution of the relative averaged intensity of temperature oscillations defined as follows,

$$\overline{\rho} = \frac{\overline{\hat{r}}}{\max(\overline{\hat{r}})} \quad , \qquad (1)$$

where,

$$\overline{\hat{r}} = \frac{1}{n}\sum_{k=1}^{n}\hat{r}_k \quad \text{and} \quad \hat{r}_k = \int_{0.1\,\mathrm{Hz}}^{0.882\,\mathrm{Hz}} |F_k(s)|^2\, ds \quad . \qquad (2)$$

Here $F_k(s)$ is the discrete Fourier-transformation of the measured temperature signal at channel k and at a given location (z,θ), and n is the number of available channels (after rejection of possible outliers) at that location.

The objective function given by Eqs. (1) and (2) was defined to describe the intensity of temperature fluctuations in frequency range from 0.1 to 1 Hz. However, due to purely numerical and signal-sampling considerations, the upper limit in the integral in Eq. (2) is taken 0.882 Hz, which is the closest possible value to 1 Hz.

Both figures consistently show that the highest relative intensity of temperature oscillations in the frequency range from 0.1 to 0.882 Hz is just below the hot inlets, which are located at z = 0.8 m. For case 1 the maximum value of $\overline{\rho}$ parameter is in the range from z = 0.75 m to z = 0.8 m, whereas for case 6 this range is from z = 0.70 m to z = 0.75 m. In both cases the parameter drops to about 0.4 to 0.6 for the axial range between z = 0.6 m and z = 0.65 m.
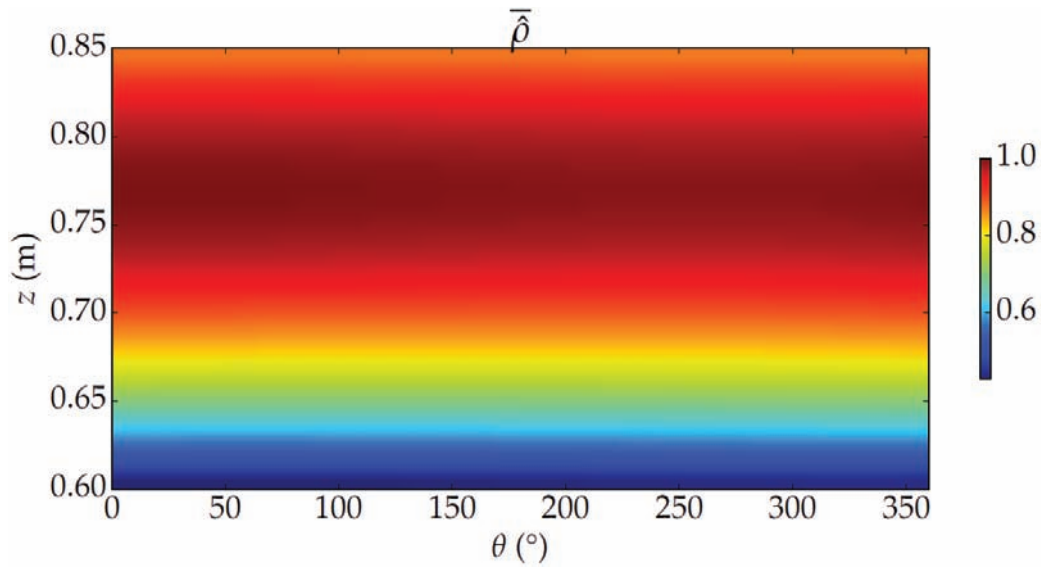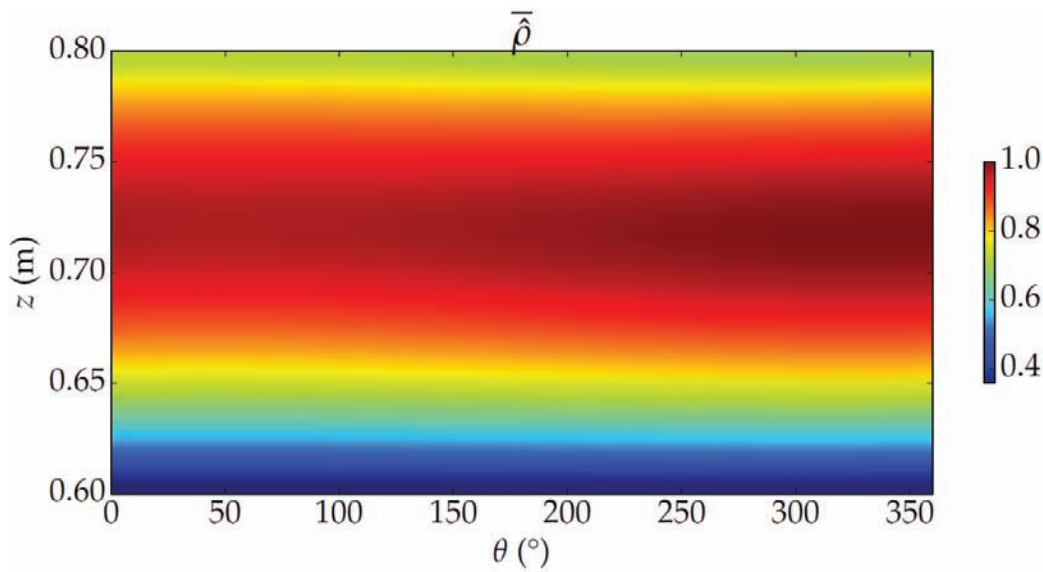
Figure 8. Relative frequency of the measured temperature fluctuations: (a) case 1; (b) case 6.

The measured results demonstrate that for the present flow arrangement large-amplitude and low-frequency (0.1 to 0.882 Hz) temperature oscillations are created. This low-frequency range has been identified as the most critical one in a sense of maximum resulting thermal stresses generated in the wall material [7-11]. Thus the present experimental data are highly relevant for thermal fatigue analysis applications in nuclear power plants.

4. CONCLUSIONS

This paper contains new experimental results on mixing of two non-isothermal water streams in an annular test section, simulating mixing region in a housing of control rods in Swedish BWRs. The operation conditions encountered in the reactor pressure vessel were created in the laboratory environment allowing for a detailed study of the mixing phenomena at high pressure (7.2 MPa) and high temperatures (333.15 to 550.15 K). The experiments show intensive temperature fluctuations in the annular mixing zone. It could be observed that the low-frequency temperature oscillations are located just below hot inlets to the test section. Such low-frequency temperature oscillations can penetrate deeply into the wall material and in advantageous conditions can lead to thermal fatigue damage of the control rod extender. Using new movable multi-sensors it became possible to obtain a large experimental database, containing wall temperature measurements at 8 azimuthal and 5 axial positions, with 13 thermocouples at each position. In total 520 temperature readings were performed, each lasting about 2 minutes and recording transient temperature with frequency of at least 100 samples per second and with an instantaneous non-calibrated uncertainty less than 3.9 K. The present experimental results can be useful to analyze the governing phenomena of the thermal fatigue and can serve as a database to validate CFD conjugate heat transfer models which are intended to be used for prediction of the thermal mixing characteristics in real reactor geometries.

REFERENCES

1. J. –A. Le Duff, A. Lefrançois, Y. Meyzaud, J. –Ph. Vernot, D. Martin, J. Mendez and Y. Lehericy, "High cycle thermal fatigue issues in PWR nuclear power plants, life time improvement of some austenitic stainless steel components," *La Revue de Métallurgie-CIT* (2007).
2. H. Tinoco, H. Lindkvist, Y. Odemark, C.-Maikel Högström and K. Angele, "Flow mixing inside a control-rod guide tube – part I: CFD simulations," proc. 18th International Conference on Nuclear Engineering, ICONE18, Xi'an, China, May 17-21, 2010, paper ICONE18-29688 (2010).
3. K. Angele, M. Cehlin, C. – M. Högström, Y. Odemark, M. Henriksson, H. Tinoco, H. Lindqvist and B. Hemström, "Flow mixing inside a control-rod guide tube – part II: experimental tests and CFD-simulations," proc. 18th International Conference on Nuclear Engineering, ICONE18, Xi'an, China, May 17-21, 2010, paper ICONE18-29689 (2010).
4. U. Meingast, L. Reichelt and U. Renz, "Measuring transient wall heat flux under diesel engine conditions," *Int. J. Engine Research*, Vol. 5, pp. 443-452 (2004).
5. L. Reichelt, U. Meingast and U. Renz, "Calculating transient wall heat flux from measurements of surface temperature," *Int. J. Heat and Mass Transfer*, Vol. 45, pp. 579-584 (2002).
6. M. Bergagio, S. Hedberg, S. Rydström and H. Anglart, "Instrumentation for temperature and heat flux measurement on a solid surface under BWR operating conditions," subm. 16th International Topical Meeting on Nuclear Reactor Thermal Hydraulics, NURETH-16, Aug. 30 – Sept. 4, 2015, Chicago (2015).
7. V. Radu, E. Paffumi, N. Taylor and K.-F. Nilsson, "Assessment of thermal fatigue crack growing in the high cycle domain under sinusoidal thermal loading. An application – Civaux 1 case," JRC Institute of Energy, Rep. EUR 23223 EN (2007).
8. IAEA-TECDOC-1361, *Assessment and management of ageing of major nuclear power plant components important to safety-primary piping in PWRs*, IAEA (2003).

9. N. Kasahara et al., Structural response function approach for evaluation of thermal stripping phenomena," *Nuclear Engineering and Design*, Vol. 212, pp. 281-292 (2002).

10. D. Buckthorpe, O. Gelineau, M.W.J. Lewis and A. Ponter, "Final report on CEC study on thermal stripping benchmark – thermos mechanical and fracture calculation, Proj. C5077/TR/001, NNC Limited (1988).

11. H.-Y. Lee, J.-B. Kim and B. Yoo, "Tee-junction of LMFR secondary circuit involving thermal, thermomechanical and fracture mechanics assessment on a stripping phenomenon, in IAEA-TEDOC-1318, *Validation of fast reactor thermomechanical and thermohydraulic codes*, IAEA (1999).